Molecular Orientation and Electronic Structure of Epitaxial Bucky Ferrocene ($Fe(C_{60}(CH_3)_5)C_5H_5$) Thin Films

Toshihiko Kaji,[†] Toshihiro Shimada*,[†] Hiroaki Inoue,[†] Yoichiro Kuninobu,[†] Yutaka Matsuo,[†] Eiichi Nakamura,*,[†] and Koichiro Saiki*,[†,‡]

Department of Chemistry, School of Science, The University of Tokyo, 7-3-1 Hongo, Bunkyo-ku, Tokyo 113-0033, Japan and Department of Complexity Science and Engineering, Graduate School of Frontier Sciences, The University of Tokyo, 7-3-1 Hongo, Bunkyo-ku, Tokyo 113-0033, Japan

Received: December 1, 2003; In Final Form: May 10, 2004

Single crystalline epitaxial films of bucky ferrocene ($Fe(C_{60}(CH_3)_5)C_5H_5$), a hybrid molecule of C_{60} and ferrocene, were grown on $MoS_2(0001)$ substrates. By using reflection high-energy electron diffraction (RHEED) amplified by a microchannel plate (MCP), it was found that the lattice constant of the film decreased from 11.3 ± 0.2 Å at 1−2 monolayer (ML) to 10.2 ± 0.2 Å at 3 ML or thicker. Both of the lattice constants were incommensurate with that of the substrate, which indicates a new type of epitaxial growth. Valence electronic structures of the films at each thickness were measured with ultraviolet photoelectron spectroscopy (UPS) and the energy levels of molecular orbitals were identified in relation to the molecular orientation in the epitaxial film.

Introduction

Various derivatives of fullerenes have been synthesized recently to explore chemical and biological functions such as molecular catalysis and gene vectors.[1] Their physical properties as new materials, however, have not been studied in detail. C_{60} is an n-type semiconductor[2−4] that is rarely found among molecular materials and several reports have been published on the fullerene as a possible component of molecular circuits.[5] Electronic functions of fullerene derivatives are thus promising and it is important to elucidate their electronic structures and properties. The problem in the study of material properties of the chemically synthesized molecules is that solvent molecules are often included in the crystalline specimen and therefore the intrinsic properties cannot be measured as synthesized. Epitaxial growth by vacuum deposition can be one of the answers to avoid the problem since the solvent molecules are usually evaporated at lower temperatures than large molecules such as fullerene derivatives and can be removed from the source prior to the deposition.

In this paper, we study the epitaxial growth and electronic structure of bucky ferrocene[6] ($Fe(C_{60}(CH_3)_5)C_5H_5$, Figure 1). The hybrid molecules between fullerenes and organometallics[6,7] are expected to exhibit unique properties because of spins in transition metals,[8,9] highly symmetric molecular orbitals, d−π interaction,[10] and electric dipoles. Since this molecule is thermally stable just as ferrocene,[11] it is expected to be vacuum sublimed by heating without decomposition. We here attempted the vacuum deposition of bucky ferrocene on a single crystalline substrate and characterized the films with reflection high-energy electron diffraction (RHEED) for the structures and ultraviolet photoelectron spectroscopy (UPS) for the valence electronic states. Information on the molecular orientation was also obtained from precise analysis of UPS.

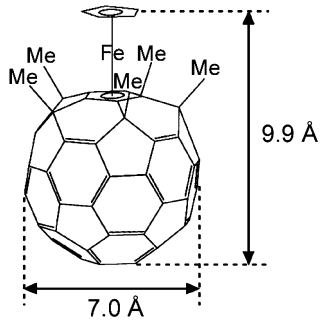

Figure 1. The molecular structure of bucky ferrocene determined by single-crystal X-ray diffraction (ref 6).

Experimental Methods

Epitaxial growth of bucky ferrocene was carried out in a UHV-chamber equipped with MCP−RHEED. Powder specimen (ca. 10 mg) of bucky ferrocene including solvents was prepared by recrystallization from toluene after the synthesis and was introduced into a sublimation source with a load-lock mechanism for the vacuum deposition. The specimen was heated repeatedly to 300 °C overnight to evaporate the solvent molecules. The degassing of the specimen started at about 200 °C and continued for several hours. A $MoS_2(0001)$ substrate (hexagonal lattice with a lattice constant of 3.16 Å) was cleaved in air just prior to the entry into the vacuum chamber and heated at 300 °C for several hours to remove surface contamination. The nominal thickness of the film was estimated from the read of a quartz crystal microbalance (QCM) taking account of the density of the bucky ferrocene and the lattice parameters obtained from RHEED analysis. The thickness was represented only in the molecular layer (ML) unit, because the lattice constant of the crystal with solvent molecules cannot be used as a reference. The growth rate was 0.1−0.3 ML/min for the source temperature of 380−420 °C. The surface morphology and orientation of the grown films were monitored by MCP−RHEED with a typical

* Address correspondence to these authors.
[†] Department of Chemistry.
[‡] Department of Complexity Science and Engineering.

10.1021/jp037668v CCC: $27.50
Published on Web 06/16/2004

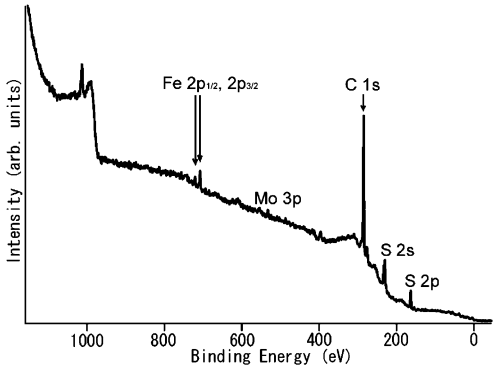

Figure 2. XPS spectra of a bucky ferrocene film measured by using MgK_α line.

incident energy of 20 keV. Diffracted electrons were amplified by a multichannel plate (MCP) to reduce the electron bombardment damage to the films.[12] UPS was measured by an angle-resolved spectrometer (Vacuum Generators ADES 400) using a He discharge source, which emits He-I ($h\nu = 21.2$ eV) or He-II ($h\nu = 40.8$ eV). We have also measured atomic force microscopy (AFM) of the films in air with a noncontact mode. X-ray photoelectron spectra (XPS) were measured using Mg Kα line on the specimen transferred via ambient condition and then annealed at 150 °C under UHV condition.

Results and Discussion

A. XPS and AFM. We measured XPS of the amorphous film of bucky ferrocene (Figure 2) to confirm the chemical stoichiometry of the thermally deposited film. The intensity ratio of C 1s to Fe 2p, corrected by the atomic sensitivity ratio of XPS[13] (0.205/3.8), was 76. This value agrees with the number ratio of C to Fe atoms in a bucky ferrocene molecule of 70 within 10%. This result strongly suggests that the molecules did not decompose after thermal evaporation. In addition to the main constituent atoms, S and Mo peaks coming from the substrate were observed. They were supposed to be signals from the cracks of MoS_2 substrate caused by the sample transfer for the XPS measurement.

Figure 3a shows the AFM image of a 0.3-ML-thick bucky ferrocene film grown at 150 °C. At the initial stage, the growth mode was layer-by-layer, because the second layer did not appear on the first layer. The coverage estimated from the AFM image was close to the nominal thickness of 0.3 ML. Figure 3b shows the AFM image of the 0.4-ML-thick film grown at room temperature (RT). The coverage of this film was estimated to be 0.3−0.4 ML, which is close to the nominal thickness. Therefore, the sticking coefficient of bucky ferrocene molecules to the MoS_2 substrate seems independent of the substrate temperature (T_s) between RT and 150 °C. However, the growth mode was much affected by T_s, because the sizes of domains of the film grown at RT are much smaller than those of the film grown at 150 °C. Figure 3c and d shows the AFM images of a 2-ML-thick film grown at 150 °C. Small domains of the second layer grow on the large first layer domains. The coverage of the 2 ML film was around 1.8 ML. Thus, the nominal thickness was considered to be correct even for the growth of the second layer. This means that the sticking coefficient did not change much between the first layer growth (heteroepitaxy) and the second layer growth (homoepitaxy). In all the AFM results above, the estimated coverage of the films ranged within 70−100% of the nominal thickness, the variation depending on the region selected for the estimation.

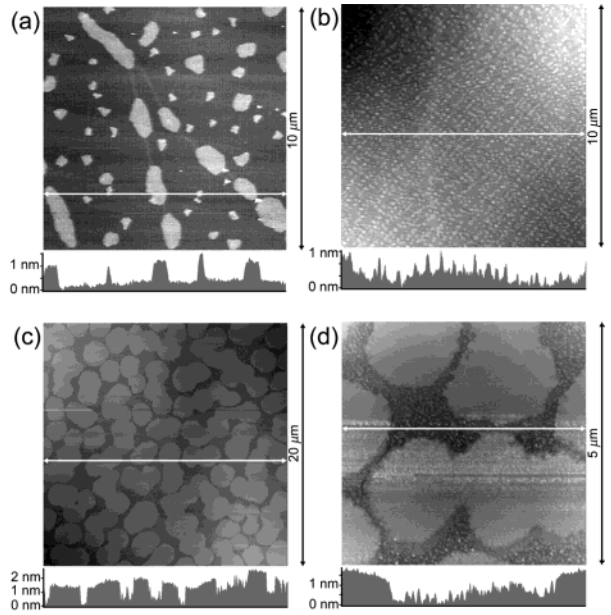

Figure 3. AFM images of a 0.3-ML-thick film (a), a 0.4-ML-thick film (b), and a 2-ML-thick film (c, d) of bucky ferrocene measured by the noncontact mode. Growth temperatures were 150 °C (a, c, d) and RT (b), respectively. The white lines in the images correspond to the positions of cross-sectional images. In a, the height of domains of the grown films (bright regions) was 0.7−1 nm.

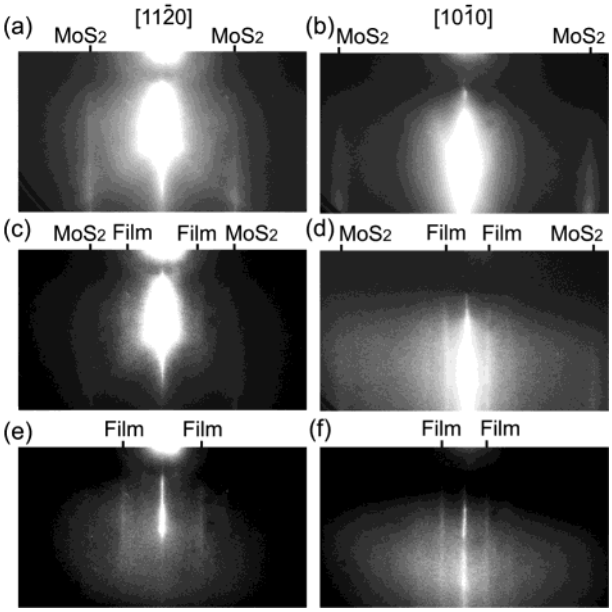

Figure 4. RHEED images of MoS_2(0001) (a, b), a 2-ML-thick film (c, d), and a 15-ML-thick film (e, f). The incident azimuths were [11$\bar{2}$0] (a, c, e) and [10$\bar{1}$0] (b, d, f) of MoS_2. "MoS_2" and "Film" denote the streaks from the substrate and the film, respectively.

B. RHEED. Figure 4 shows RHEED images of MoS_2(0001) (a, b), a 2-ML-thick film (c, d), and a 15-ML-thick film (e, f). The substrate temperature during the growth was 150 °C. In Figure 4c and d, new streaks originating from the film appeared between the streaks from a MoS_2 substrate. These patterns indicate that a single crystalline film of bucky ferrocene grew epitaxially on a MoS_2 substrate and that the planar lattice of the film was approximately hexagonal $2\sqrt{3} \times 2\sqrt{3}$ $R30°$ structure as shown in Figure 5, although the lattice of bucky ferrocene was slightly incommensurate with the substrate lattice. With an increasing film thickness, background intensity of RHEED images increased and the image eventually became a

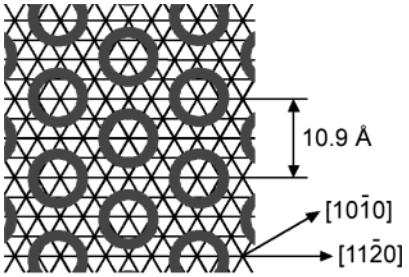

Figure 5. The planer lattice of a $MoS_2(0001)$ substrate (lines) and a bucky ferrocene film (open circles). The lattice of bucky ferrocene was approximately $2\sqrt{3} \times 2\sqrt{3}$ *R*30°, although the lattice constant slightly changes from 10.9 Å ($=2\sqrt{3}$ of the lattice constant of $MoS_2(0001)$) depending upon the thickness.

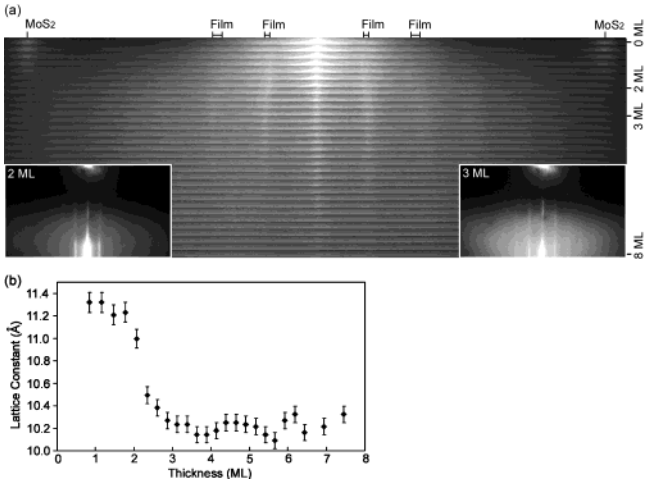

Figure 6. (a) Montage of the RHEED images measured during the film growth. The incident azimuth was parallel to [10$\bar{1}$0] of $MoS_2(0001)$. Insets show the RHEED images of a 2-ML-thick film (left) and a 3-ML-thick film (right). (b) The change of the lattice constant of the film depending on the thickness.

halo pattern. For the films grown at 150 °C, the streak patterns continued to be observed until 30 ML thickness. For the films grown at room temperature, however, the RHEED image soon became very dim and almost unobservable even at 7 ML.

In Figure 4, the spacing of the streaks became larger for thicker films. We have recorded the RHEED patterns during the thin film growth at a certain interval to examine the change in the lattice constants precisely as a function of film thickness. Figure 6a shows the RHEED images during the film growth observed with the incident azimuth parallel to [10$\bar{1}$0] of the MoS_2 substrate. Each horizontal stripe corresponds to diffraction around a constant momentum transfer along the surface normal. They were arranged from the top to the bottom in accordance with a constant increase of the deposited material. The top stripe corresponds to the diffraction of the substrate before the deposition, and the bottom stripe corresponds to the diffraction from the 8-ML-thick film. The spacing between streaks remained constant within an experimental error beyond 8 ML and the pattern becomes gradually dim when the thickness was increased further. Figure 6a clearly shows the lattice constant of the film changed suddenly during the film growth. The lattice constant of the film obtained from Figure 6a is shown in Figure 6b as a function of the thickness. A drastic change from 11.3 $\pm$ 0.2 Å to 10.2 $\pm$ 0.2 Å is observed when the nominal thickness was increased from 2 to 3 ML.

The change in the lattice constant of the films is typically found in pseudomorphic growth in which the interfacial strain induced by the commensurate relation between the film and the substrate is released as the thickness is increased.[14] For example, the lattice of a C_{60} film grown on a GaAs(001) substrate can be expanded because of the interfacial strain by as large as 13%.[15] The present result, however, cannot be explained by this mechanism because of the following reasons. If the lattice with an original lattice constant is strained because of the commensuration to the substrate, the lattice constant at the interface must be between the original value and the commensurate value. In the present case, the nearest lattice constant commensurate to the MoS_2 lattice (3.16 Å) is 10.9 Å ($2\sqrt{3} \times 2\sqrt{3}$ *R*30°). Thus, taking 10.2 Å (the observed lattice constant for 3 ML or thicker films) as the original lattice constant, the lattice constant at the interface must be 10.2−10.9 Å. However, the observed lattice constant of 11.3 Å is out of this range even with the experimental error. We examine the origin of this change in relation to the molecular orientation in the following.

It is very difficult to estimate the molecular orientation from the RHEED intensity data, because the information along the surface normal is smeared out in the surface diffraction. In the lattice structures determined above, a molecule is regarded as a point without internal structure. We here attempt to construct a model that accounts for the lattice structures obtained from RHEED. We first consider the molecular orientation in the film with the thickness of 3 ML or larger, because the explanation is simpler than the case of 2 ML or lower. The lattice constant of 10.2 Å, which was observed at 3 ML or larger, is close to the intermolecular distance in C_{60} single crystals (10.0 Å)[16] and the lattice constant of a C_{60} film grown on a $MoS_2(0001)$ substrate (10.0 $\pm$ 0.2 Å).[17,18] Taking account of the molecular size of the bucky ferrocene (see Figure 1), the distance between adjacent fullerene cages is 3.2 Å, because the intermolecular distance is 10.2 Å and the diameter of the cages is 7.0 Å. This value of 3.2 Å is appropriate for the van der Waals distance between molecules. This analysis strongly suggests that the long axes of the molecules are aligned perpendicular to the surface.

In 2 ML or lower, the lattice constant of the film was 11.3 Å, which indicates the long axes of the molecules are more inclined from the surface normal than in the films with 3 ML thickness or larger. The mechanism of the inclination can be due to an entropy effect that causes free rotation of the molecules as reported in fcc-C_{70}.[19−21] C_{70} molecules show anisotropic rotation and give random orientation on average because of an entropy effect. There is also a possibility that the attracting van der Waals interaction between the π-orbitals of the molecule and the substrate makes the long axis tilted to the surface plane. Molecular rotation must be involved also in this case to account for the observation of hexagonal lattice.

Next, we speculate on the mechanism of the change in the molecular orientation. When the long axes of the molecules are aligned in the films thicker than or equal to 3 ML, two cases can be considered on the orientation of adjacent molecules, that is, parallel or antiparallel. We here consider the dipole moment of the molecule. In ref 11, the ^{1}H and ^{13}C NMR results suggest that the fullerene core withdraws an electron from the ferrocene moiety. We estimated[22] that the dipole moment was 5.55 D by density functional calculation using B3LYP/6-31G(d). If the molecules have dipole moments as in the present case, antiparallel orientation should be energetically favorable. In the planar hexagonal lattice structure, nesting of two rectangular lattices with antiparallel orientations (Figure 7) is the simplest arrangement to satisfy this condition. This lattice structure has been actually observed in the crystals of C_{60} derivatives "shuttlecock fullerenes".[23,24] Thus, the driving force to change

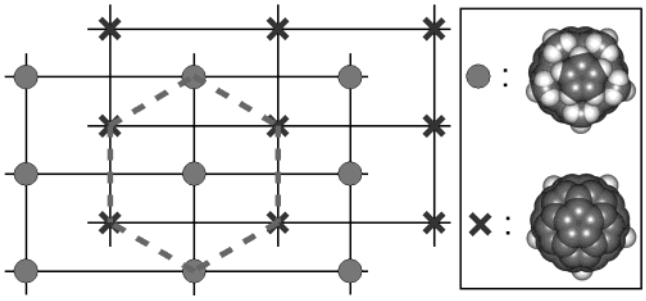

Figure 7. Model of the structure of 3 ML or thicker films. A hexagonal lattice consists of nesting of two rectangular lattices. In each rectangular lattice, all the molecules are oriented to the same direction perpendicular to the lattice. The molecules in the other lattice are aligned to the opposite direction. Two orientations of the molecules are illustrated in the box.

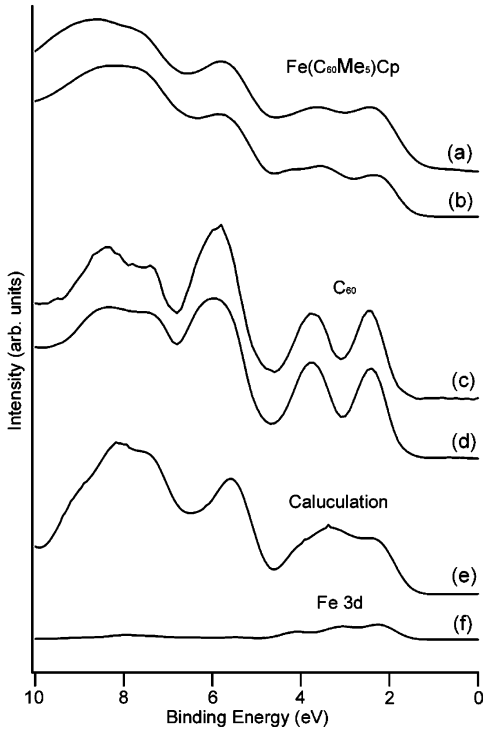

Figure 8. UPS spectra of an epitaxial film (15-ML-thick) grown at 150 °C (a, b) and an epitaxial film of C_{60} (10-ML-thick) (c, d). The photon energies for the UPS are 40.8 eV (He-II) (a, c) and 21.2 eV (He-I) (b, d). The valence density of states of a whole molecule (e) and the contribution of Fe 3d orbitals (f) calculated by B3LYP/6-31G(d).

the molecular orientation from the disordered orientation due to the rotation of the molecules in the thinner films to the aligned orientation in the thicker films may be this stabilization from the antiparallel alignment of the dipole moments.

C. UPS. Since we have prepared thin films without solvent molecules, we measured UPS of bucky ferrocene thin films to study the electronic structure of the material. Figure 8 shows the UPS of an epitaxial film of bucky ferrocene (15-ML-thick) grown at 150 °C (a, b), an epitaxial film of C_{60} (10-ML-thick) (c, d), and valence density of states calculated[22] by B3LYP/6-31G(d) (e, f). The calculated spectra were obtained by summing up the contribution from the discrete energy levels with Gaussian broadening of 0.4 eV. The calculated spectra are shifted by −3.4 eV to make a best fit between the total density of states (e) and the experiment since the position of the energy levels can be different from the experimental ones because of intermolecular interaction and final state effects in UPS. The photon energies

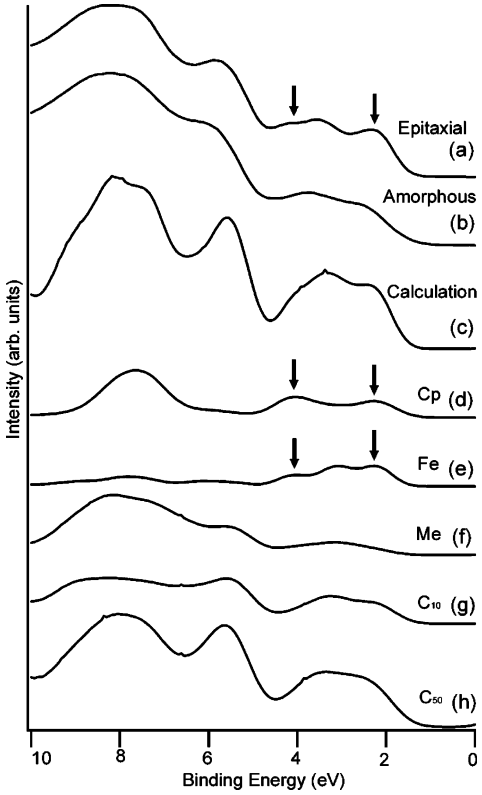

Figure 9. UPS spectra of an epitaxial film (15-ML-thick) (a) and that of an amorphous film (24-ML-thick) (b) grown on $MoS_2(0001)$ measured with $h\nu = 21.2$ eV. The others show the calculated valence density of states from the whole molecule (c) and the contributions of Cp (d), Fe (e), Me (f), C_{10} (a part of C_{60} cage facing the Fe atom) (g), and the bottom C_{50} cage (h).

for the UPS are 40.8 eV (He-II) and 21.2 eV (He-I) for Figure 8a, c and b, d, respectively. In the calculation, total density of states is shown as Figure 8e while the contribution from Fe 3d orbitals is shown as Figure 8f. By comparing spectra of bucky ferrocene with that of C_{60}, two features are noticed. (i) Bucky ferrocene shows broader peaks than C_{60}, and (ii) the relative intensity of binding energy (E_B) range between 2 and 5 eV is stronger in the spectrum measured at $h\nu = 40.8$ eV than that measured at $h\nu = 21.2$ eV. In the calculated density of states, the chemical species having strong intensities specifically in this region is Fe 3d as seen in Figure 8f. This result is consistent with the well-known tendency that the cross section of photoemission from d orbitals becomes larger than that from s or p orbitals when photon energy is increased.[25]

Next, we discuss the molecular orientation from UPS of the films with different crystallinity. Figure 9a, b shows UPS of an epitaxial film (15-ML-thick) and that of an amorphous film (24-ML-thick) grown on $MoS_2(0001)$ measured with $h\nu = 21.2$ eV. The crystallinity was controlled by changing the growth temperature (150 °C for an epitaxial film and RT for an amorphous film). Differences are found in the spectra at $E_B \sim 4.1$ eV, in which only the epitaxial film shows a peak, and at $E_B \sim 2.3$ eV, in which the epitaxial film shows a peak stronger than that of the amorphous film. To identify the origin of the peaks, we show the calculated valence density of states from the whole molecule (c), Cp (d), Fe (e), Me (f), C_{10} (a part of C_{60} cage facing to the Fe atom) (g), and the bottom C_{50} cage (h) in Figure 9. It is concluded from the calculation that the peak at 4.1 eV corresponds to Cp and Fe. The peak at 2.3 eV also corresponds to the peaks in the calculated spectra of Cp and Fe, although there are shoulders at 2.3 eV in the calculated spectra of C_{10} and C_{50}. Since the probing depth of He-I UPS is

comparable to the size of the molecule, this result strongly suggests that much more Cp exists at the topmost surface in the epitaxial film than in the amorphous film, in which molecules are supposed to be oriented randomly. It is consistent with the model structure derived from the RHEED measurement, in which the long axes of the molecules are aligned perpendicular to the substrate surface when the thickness is 3 ML or larger.

Conclusions

We have grown epitaxial films of bucky ferrocene on MoS_2(0001) substrates. Precise RHEED observation revealed that the surface lattice constant of the films was 11.3 ± 0.2 Å when the thickness was 2 ML or lower and it changed to 10.2 ± 0.2 Å at 3 ML. It is probably due to the orientational change of the molecules, in which the long axes of the molecules rotate randomly at first and then changes the orientation so as to align the long axes perpendicular to the surface. We have also measured UPS of the films and the result was consistent with the above orientation in thick epitaxial films because the peaks originating from Cp and Fe are enhanced in thick epitaxial films whereas the peak is negligible in the amorphous films.

Acknowledgment. This work was supported by Grant-in-Aid for Creative Scientific Research (14GS0207) and by The 21st Century COE Program for Frontiers in Fundamental Chemistry from the Ministry of Education, Culture, Sports, Science, and Technology.

References and Notes

(1) Nakamura, E.; Isobe, H. *Acc. Chem. Res.* **2003**, *36* (11), 807−815.

(2) Haddon, R. C.; Perel A. S.; Morris, R. C.; Palstra, T. T. M.; Hebard, A. F.; Fleming, R. M. *Appl. Phys. Lett.* **1995**, *67* (1), 121−123.

(3) Horiuchi, K.; Nakada, K.; Uchino, S.; Hashii, S.; Hashimoto, A.; Aoki, N.; Ochiai, Y. *Appl. Phys. Lett.* **2002**, *81* (10), 1911−1912.

(4) Kobayashi, S.; Takenobu, T.; Mori, S.; Fujiwara, A.; Iwasa, Y. *Appl. Phys. Lett.* **2003**, *82* (25), 4581−4583.

(5) Park, H.; Park, J.; Lim, A. K. L.; Anderson, E. H.; Alivisatos, A. P.; McEuen P. L. *Nature* **2000**, *407*, 57−60.

(6) Sawamura, M.; Kuninobu, Y.; Toganoh, M.; Matsuo, Y.; Yamanaka, M.; Nakamura, E. *J. Am. Chem. Soc.* **2002**, *124*, 9354−9355.

(7) Matsuo, Y.; Nakamura, E. *Organometallics* **2003**, *22* (13), 2554−2563.

(8) Barraclough, C. G.; Martin, R. L.; Mitra, S.; Richard C. *J. Chem. Phys.* **1970,** *53* (5), 1638−1642.

(9) Yamada, H.; Shimada, T.; Koma, A. *J. Chem. Phys.* **1998**, *108*, 10256−10261.

(10) Hünig, S.; Erk, P. *Adv. Mater.* **1991**, *3* (5), 225−236.

(11) Nakamura, E. *Pure Appl. Chem.* **2003**, *75* (4), 427−434.

(12) Saiki, K.; Kono, T.; Ueno, K.; Koma, A. *Rev. Sci. Instrum.* **2000**, *71* (9), 3478−3479.

(13) Wagner, C. D.; Riggs, W. M.; Davis, L. E.; Moulder J. F. In *Handbook of X-ray Photoelectron Spectroscopy;* Muilenberg, G. E., Ed.; Perkin-Elmer: Eden Prairie, MN, 1979.

(14) Pimpinelli, A.; Villain, J. *Physics of Crystal Growth;* Cambridge University Press: Cambridge, U.K., 1998.

(15) Sakurai, T.; Xue, Q.; Hashizume, T.; Hasegawa, Y. *J. Vac. Sci. Technol., B* **1997**, *15* (5), 1628−1632.

(16) Krätschmer, W.; Lamb, L. D.; Fostiropoulos, K.; Huffman, D. R. *Nature* **1990**, *347*, 354−358.

(17) Sakurai, M.; Tada, H.; Saiki, K.; Koma, A. *Jpn. J. Appl. Phys.* **1991**, *30* (11A), L 1892-L 1894.

(18) Sakurai, M.; Tada H.; Saiki, K.; Koma, A.; Funasaka, H.; Kishimoto Y. *Chem. Phys. Lett.* **1993**, *208* (5, 6), 425−430.

(19) Tycko, R.; Haddon, R. C.; Dabbagh, G.; Glarum, S. H.; Douglass, D. C.; Mujsce, A. M. *J. Phys. Chem.* **1991**, *95*, 518−520.

(20) Vaughan, G. B. M.; Heiney, P. A.; Fischer, J. E.; Luzzi, D. E.; Ricketts-Foot, D. A.; McGhie, A. R.; Hui, Y.-W.; Smith, A. L.; Cox, D. E.; Romanow, W. J.; Allen, B. H.; Coustel, N.; McCauley, J. P. Jr.; Smith, A. B., III. *Science* **1991**, *254*, 1350−1353.

(21) Sprik, M.; Cheng, A.; Klein, M. L. *Phys. Rev. Lett.* **1992**, *69* (11), 1660−1663.

(22) *Gaussian 03*, Revision B.02; Gaussian, Inc.: Pittsburgh, PA, 2003.

(23) Sawamura, M.; Kawai, K.; Matsuo, Y.; Kanie, K.; Kato, T.; Nakamura, E. *Nature* **2002**, *419*, 702−705. (The intermolecular distance in the crystals of the molecules is larger than the 10.2 Å value (14.2−17.2 Å), as they contain solvent molecules within the crystal lattice.)

(24) Matsuo, Y.; Muramatsu, A, Hamasaki, R.; Mizoshita, N.; Kato, T.; Nakamura, E. *J. Am. Chem. Soc.* **2004**, *126*, 432−433.

(25) Yeh, J. J.; Lindau, I. *Atomic data and Nuclear Data Tables* **1985**, *32* (1), 1−155.